



Outflow characterization of a transpiration cooled fin for the sounding rocket experiment HIFLIER 1

Jonas Peichl, Giuseppe Di Martino, Markus Selzer³

Abstract

This paper presents a study on the outflow characteristics of a sharp edged, transpiration cooled fin as flown as part of the FinEx experiment of the HIFLIER1 sounding rocket. The permeable ceramic matrix composite material used for the transpiration cooled leading edge shows in general a relatively homogeneous outflow pattern disrupted by significant strong jets caused by small inhomgeneities. The general strongly anisotropic outflow characteristics were also investigated. The findings of the outflow characterization led to valuable insights for the design of future sharp edged transpiration cooled structures

Keywords: Transpiration cooling, Ceramic Matrix Composites, Thermal Protection Systems

Nomenclature

Latin ρ – density

a – distance perpendicular to surface μ – dynamic viscosity

A – Area Subscripts

K - Permeability coefficient l, L - length amb - ambient

 \dot{m} — mass flow rate c — characteristic p — pressure dyn — dynamic T — Temperature D — Darcy

u – velocity F – Forchheimer

Greek in – Conditions at inlet α – angle relative to surface out – Conditions at inlet

1. Introduction

The thermal protection of the external structures represents one of the most challenging requirements for the development of hypersonic flight vehicles, since they are exposed to the harsh thermal loads determined by the forming highly-energetic shock waves, especially at sharp-edged structures [1, 11]. Typically, these requirements lead to the application of lightweight ceramic matrix composites (CMC), such as C/C-SiC, for thermal protection systems, as they are able to withstand high temperatures. In this framework, the Institute of Structures and Design of the German Aerospace Centre (DLR-BT) has developed a unique expertise for the development of such materials , its full characterization as well as the integration and validation as a thermal protection system (TPS) for hypersonic sounding rocket flight experiments, successfully flown for example in SHEFEX I and II [12, 26] and most recently in STORT [10]. Moreover, the usage of this material for stabilizer fin structures could be successfully demonstrated in the FinEx experiment on the HiFire-5 flight experiment [3]. However, in order to overcome

¹Research Scientist, DLR Institute of Structures and Design, Pfaffenwaldring 38-40, 70569 Stuttgart, Germany, Jonas.Peichl@dlr.de

²Research Scientist, DLR Institute of Structures and Design, Pfaffenwaldring 38-40, 70569 Stuttgart, Germany, Giuseppe.DiMartino@dlr.de

³Research Scientist, DLR Institute of Structures and Design, Pfaffenwaldring 38-40, 70569 Stuttgart, Germany Markus.Selzer@dlr.de

the load limits, in the cases in which the heat fluxes become even more critical, active cooling of the structure could become necessary, e.g. for flight at high Mach numbers or for longer flight endurance. In this framework, one of the possibilities is represented by the usage of transpiration cooling, which works by feeding a coolant fluid through a porous wall into the hot gas region, with the double effect of directly cooling the wall itself and mixing into the boundary layer resulting in a lower convective heat flux on the structure. In order to combine the application of CMC structures with the transpiration cooling technology, suitable CMC materials have to be used. For past fundamental investigations on transpiration cooling using CMC materials, Carbon fiber reinforced Carbon (C/C) was used, e.g. in [17, 21, 2]. However, the low oxidation resistance of C/C led at DLR-BT to the development of the so-called OC-TRA (Optimized Ceramic for Transpiration Cooling Application) material [8], which consists in a variant of the C/C-SiC CMC material with defined porosity level designed specifically for transpiration cooling applications.

Transpiration cooling relies on a relatively homogeneous outflow of the coolant, as inhomogeneities like pore blockages lead to hot spots, as shown e.g. by Liu et al. [18]. These hot spots could potentially compromise the structural integrity of the thermal protection system. As the materials used for transpiration cooling are not perfectly homogeneous and real-word designs might have large blockages like fasteners and sensors integrated in the structure, the knowledge of the outflow pattern can serve as a boundary conditions for the prediction of the temperature of the transpirational cooled structure through computational fluid dynamics simulations. König et al. [16] found for the cooled wall temperature a good agreement of between experimental data and numerical simulations when using a non-uniform mass flow boundary condition derived from outflow pattern measurements. Furthermore, large fluid jets might trigger an early boundary layer transition or lead to cooling film separation [14]. For the characterization of the outflow pattern, two methodologies are being used. To characterize the outflow pattern of transpiration cooled ultra-high temperature ceramics, Ifti et al. [14] employed miniature-hot wire anemometry, in order to determine the local outflow velocity. A similar approach was taken by Gulli and Maddalena, using hot-wire anemometry[13]. However, as this method enables only a relatively low resolution of the outflow pattern, the outflow pattern can also be determined using a movable pitot tube, as it will be presented in the following paper. For such measurements, the AORTA (Advanced Outflow Research facility for Transpiration Applications) test bench developed at DLR-BT, has been extensively used for characterizing different permeable materials such as CMC flat samples and cones [16, 9], additively manufactured metals [20] and porous rocket engine injector elements [23]. However, these investigations were performed on simple geometries for fundamental investigations, while in this paper, a study on transpiration cooled structures as used on a flight experiment will be presented.

In order to assess the performance of transpiration cooled sharp edged structures under hypersonic flight conditions, in the framework of the flight experiment project Hypersonic International Flight Research Experimentation (HIFLIER), coordinated by the US Air Force Research Laboratory (AFRL) and operated by DLR's Mobile Rocket Base (DLR-MORABA) an experimental module (so called FinExII) of the sounding rocket has been designed and constructed by DLR-BT, in collaboration with the High Enthalpy Flow Diagnostic group (HEFDiG) of the Institute of Space Systems (IRS) at the University of Stuttgart. The module contained four sharp-edged fins, with two of them being transpiration cooled an two fins acting as uncooled reference.

The HIFLIER1 sounding mission rocket has successfully launched on the 10th October 2023 from the Esrange Space Center in Kiruna (Sweden), providing valuable insights on the performance of a transpiration cooled fin under hypersonic flight conditions. For details on the design of the flight experiment and the respective results from the flight campaign, the authors refer to [4, 5, 6, 7]

This paper aims to present the through flow and outflow characteristics of a fin as the ones uses on the FinEx transpiration cooling experiment on the HIFLIER1 sounding rocket. The determined characteristics are determined for an undisturbed environment, neglecting effects existent in the flight experiment caused by external effects, such as pressure gradients distributed over the fin surface.

2. Experimental Setup

In the following, a brief description of the investigated fin is given, which has the same design as the fins flown on the HIFLIER flight experiment. Furthermore, the experimental test bench for permeability and outflow investigations is described.

2.1. Description of investigated fin

The investigated fin is made of the so-called OCTRA material, which is a permeable version of the typically used C/C-SiC material. While classical C/C-SiC material produced via liquid silicon infiltration is almost impermeable, OCTRA is obtained by including a predefined amount of aramid fibers in the carbon-fiber reinforced plastic (CFRP) preform. The aramid fibers thermally degrade during pyrolysis generating larger pores which are not completely filled during the silicon infiltration. In this way, the permeability level can be defined based on the amount of aramid fibers included in the CFRP preform. More info on the OCTRA material, the manufacturing process, and the characterization of the main material properties can be found in [8].

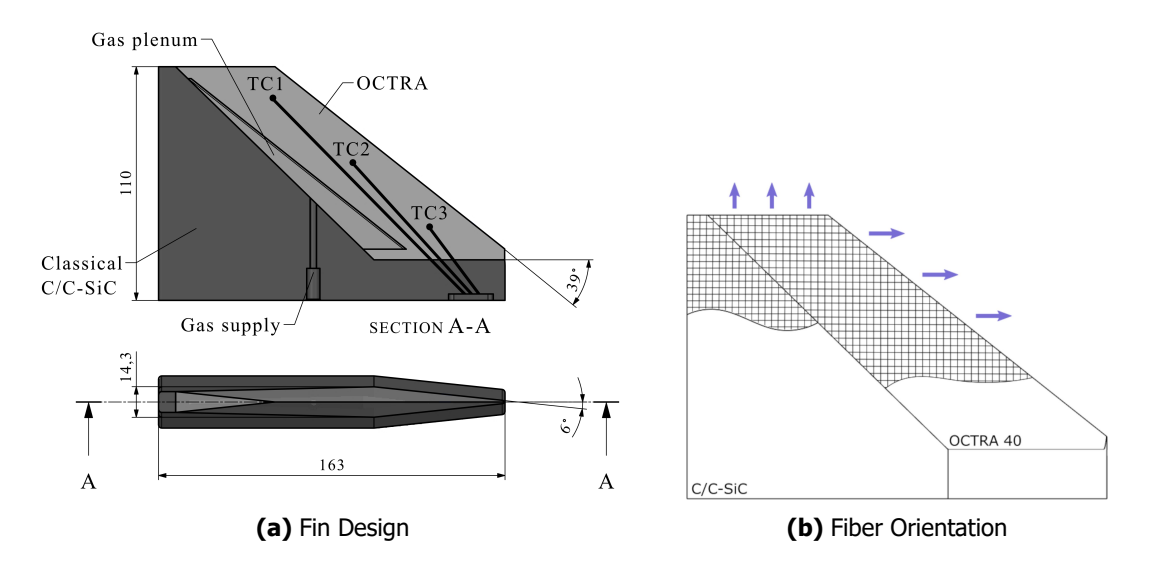


Fig 1. Description of the investigated Fin

Figure 1 shows the overall design of the CMC fin. The highest aerothermal loads and consequently temperatures are expected at the leading edge. In order to concentrate the cooling in thie region of the leading edge, where the higher aerothermal loads and consequently high temperatures are expected, only the forward part of the fin is made of the permeable OCTRA material (displayed in light grey in Figure 1a), while the remaining part is made of classical impermeable C/C-SiC (in dark grey in Figure 1a). Taking into account that in the manufacturing process of the OCTRA material the main orientation of the pores is determined by the direction of the aramid fibers in the CFRP precursor, which was produced using two-dimensional mixed carbon/aramid fiber plies resulting in a objected main orientation of the pores parallel to the chosen fiber orientation, as shown in Fig.1b. Moreover, in the present work the OCTRA40 variant of the material was adopted, indicating a 40% vol percentage of aramid fibres fibers in the CFRP preform leading to a porosity of around 8-9% in the final C/C-SiC state. The fin in its final state is shown in Fig.2.



Fig 2. Picture of investigated fin

2.2. AORTA test facility

The AORTA test bench used in the following study was designed for the characterization of porous materials regarding their permeability and outflow distribution. Therefore, porous samples or components can be perfused by gaseous nitrogen with mass flows from 0.02 g/s to 12 g/s at pressures up to 15 bar. The mass flow rates, pressures and temperatures are recorded. With these measurements, the permeability can be determined, describing the pressure loss of the fluid flow through the porous medium. This permeability is usually expressed by the Darcy-Forchheimer equation, which is in the formulation by Innocentini et al. [15] describes the pressure loss of a fluid through a porous medium as

$$\frac{p_{in}^2 - p_{out}^2}{2p_{out}L_c} = \left(\frac{\mu}{K_D}\right)u_D + \left(\frac{\rho}{K_F}\right)u_D^2 \tag{1}$$

where p_{in} and p_{out} are the coolant gas pressure at the inlet and outlet of the porous medium respectively, μ and ρ are its viscosity and density, L_c is the characteristic length of the porous medium and K_D and K_F are the Darcy and Forchheimer coefficients. The superficial Darcy velocity u_D can be derived from the coolant mass flow rate \dot{m} via the continuity equation

$$u_D = \frac{\dot{m}}{\rho A_c} \tag{2}$$

where A_c is the outflow area. The facility is made up of three parallel gas lines, which can be opened and closed by pneumatically driven valves. Each line includes a Bronkhorst CORI-FLOW mass flow controller M12, M14 and M55 respectively, each optimized for a certain range of mass flow rates. P33X-series pressure gauges for 300 bar and ambient pressure (0.8 bar-1.2 bar) with an uncertainty of 0.05% are used to measure the inlet and outflow pressures at steady state conditions for different values of the cooling gas mass flow rate. Furthermore type-K thermocouples are used to measure the respective inlet and outflow temperatures. K_D and K_F are then obtained by fitting the measured data according to Eq. 1, using a least squares algorithm.

Additionally, the outflow distribution of the porous material can be characterized by measuring dynamic pressures via pitot tubes mounted on linear axes. To measure the outflow distribution, the pitot tube is moved over the sample and stationary pressure measurements are automatically done. This allows for an automated, detailed measurement of the outflow characteristics as will be shown in the current report. During the measurement a pitot tube is moved by high precision linear units (positional accuracy $< 10 \, \mu m$) driven by step motors. The sensor is moved in a meander pattern over the sample and the control software automatically acquires stationary dynamic pressure values for each point as the mean value over 20 measurements. For the outflow measurements, two different pitot tubes with inner diameters of 0.8 mm and 0.3 mm have been used, both connected to a pressure transducer PTSXR from

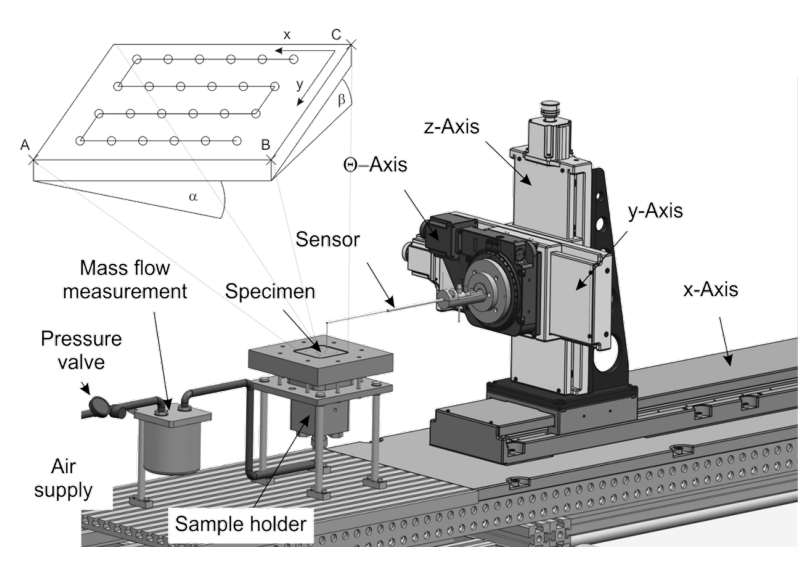


Fig 3. Test setup and measurement procedure

Airflow Lufttechnik GmbH with a maximum pressure of $1000 \, \text{Pa}$. The sensor inherited uncertainty for the measurement chain amounts to $7 \, \text{Pa}$. The mass flow is measured by a M14 Coriolis with an uncertainty below $0.5 \, \%$.

Another important parameter for the measurements is the distance from the pitot tube to the sample. This distance is determined by moving the pitot tube in increments of $1/100\,\mathrm{mm}$ to the sample until a consistent electrical contact can be measured. To take into account the roughness of the sample, a small metallic plate with a thickness of 1 mm is placed on the sample for these measurements. The repeatability of this measurement is typically \pm $1/100\,\mathrm{mm}$. Also, with measurements of 4 points on the sample plane, the sample plane is also aligned to the x-y-plane of the sensor, with deviations in height of these points below $7/100\,\mathrm{mm}$ during the shown measurements.

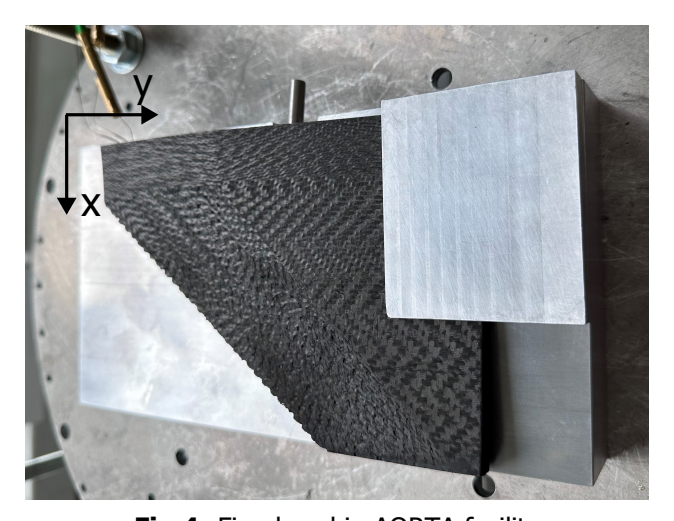


Fig 4. Fin placed in AORTA facility

Often the flow through a porous medium is assumed to be homogeneous and an average velocity is used to describe the porous flow. However, on a pore scale, the flow is made up of several fluid jets flowing out of the pores and regions with no outflow between the pores. Depending on the size of the pitot tube compared to the pore size and distribution, it is obvious, that the measured distribution already contains some sort of averaging. Besides this averaging, additional errors are induced by the pitot tube

disturbing the flow. Thus, the absolute measured pressure values are distorted and should not be taken as the true values. This was already described in [23, 22, 25, 24]. Nonetheless, the measurements are able to differentiate between regions with flow, e.g. pores, and regions without flow and higher pressure values correlate to higher velocities and thus higher mass flow.

Fig. 4 shows the fin placed in the AORTA facility, with the orientation to the absolute coordinate system of the facility. The fin is held in position by a milled sample holder, allowing the port side flank of the permeable leading edge to be aligned to the xy-plane of the facility.

3. Results of Fin Permeability Characterization

The characterization of the permeability was first performed on a cylindrical sample taken from the same OCTRA material batch from which the fins' leading edges have been manufactured, as described in [4]. Then, a measurement was taken of the investigated fin. Steady-state pressure measurements were conducted by feeding the specified gaseous nitrogen mass flow rate in the range 0-1.5 g/s gaseous nitrogen. The determined Darcy and Forchheimer coefficients are given in Table 1. For the calculation of K_D and K_F , the outflow area was considered as the projected area of the leading edge, with $A_c = 2.69 \cdot 10^{-3} \text{ m}^2$. Furthermore, a characteristic length of $L_c = 38 \text{ mm}$ was assumed. Note, that

Parameter	Symbol	Unit	reference cylindrical [4]	Fin
Darcy Coefficient	K_D	m ²	1.62·10 ⁻¹²	1.82-12·10 ⁻¹²
Forchheimer Coefficient	K_F	m	4.5·10 ⁻⁷	2.67·10 ⁻⁸

Table 1. Permeability coefficients measured

for the cylindrical samples, only flow into one direction in the fiber plane is allowed, as rubber sealing prevents lateral flow. As already described in [19], the OCTRA material can be considered as practically impermeable for flow perpendicular to the fiber plane.

4. Results of Outflow Measurements

In the following, the results of the outflow characterization are presented. All presented outflow measurements were performed using a nitrogen mass flow rate of 2 g/s and a pitot probe with an orifice diameter of 0.8 mm. In order to create a significant overlap between the single measurements, a step size of 0.4 mm was chosen, resulting in a measurement density of 625 Pt/cm².

All measurements have been taken at ambient conditions $p_{amb} \approx$ 0.96 bar and $T_{amb} \approx$ 295 K.

4.1. Characterization of the anisotropic outflow characteristics

Due to the highly anisotropic structure of the OCTRA material as shown in Section 2.1, a significant directional dependency is expected, with a main outflow direction parallel to the carbon fiber plies. Therefore, a detailed investigation of the directional outflow characteristics was performed.

The measurements in the following subsection were performed taking 20x20 measurements with an step with of 0.4 mm, resulting in an 8 mm x 8 mm measurement window. The position chosen was in the center of the fin, as being as representative as possible for the general outflow behavior. In Fig. 5, the outflow distribution of the characterized area is shown, with different distances to the fin surface. The measurements shown are taken at l=0.3 mm, 1 mm, 2 mm and 3 mm, respectively. For these measurements, a constant α = 90° was kept. The overall outflow distribution can be characterized, especially close to the fin surface, by a medium- to low level dynamic pressure field, with a small number of single high pressure jets. With a higher distance to the respective pore, the average dynamic pressure decreases significantly. By assuming the outflow of a pore as a turbulent jet, the flow profile of a single jet widens radially, with an decrease in velocity, leading to lower dynamic pressures. This effect could be already demonstrated on perfused RIGIMESH samples using the same facility by Selzer et al. [23]. Exemplary, an interesting, behavior can be observed in the lower right corner of Fig.5b-5d. In Fig. 5b, two discrete jets get visible. With rising distance to the fin surface (Fig. 5c and Fig. 5d, the observed jets are widening, which is accompanied by a decrease in the measured peak dynamic pressure. Furthermore, the position of the jet shifts slightly in direction of the leading edge

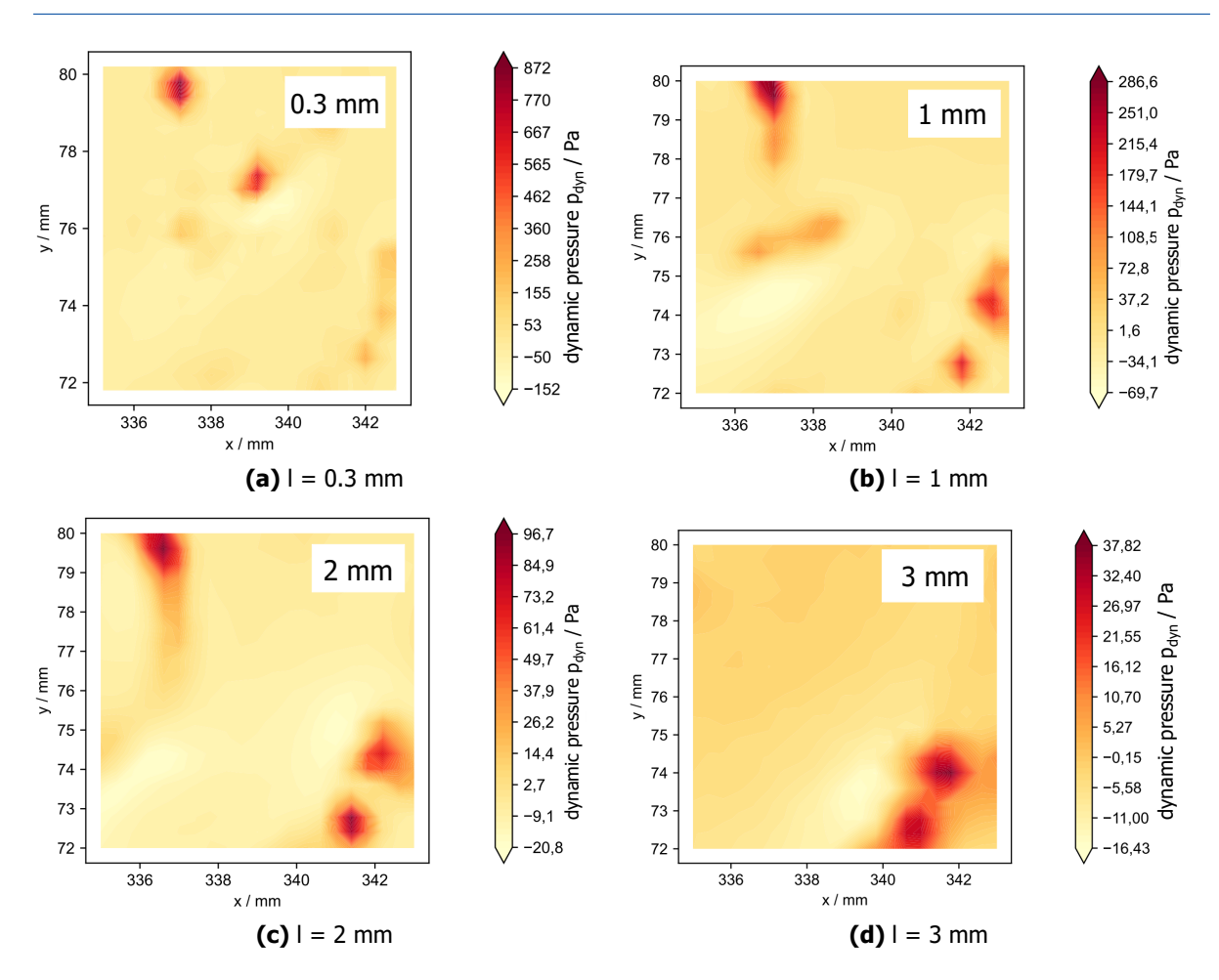


Fig 5. Outflow distribution with different surface-probe distances

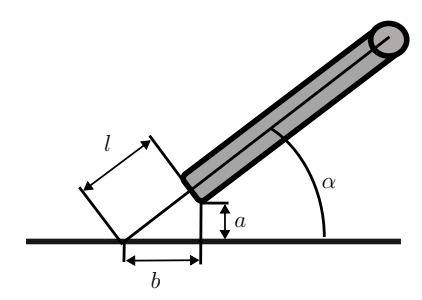


Fig 6. Angle Definition

(negative x-direction). This indicates, that the observed jets are not perpendicular to the fin surface, but rather inclined. For further investigations of the inclination of jets, an investigation of the the same measurement window, but with different inclinations relative to the fin surface was performed. Due to geometric constraints of the pitot tube, it is not possible to measure the outflow exactly aligned to the assumed main outflow plane. The geometrical situation is shown in Fig.6. The aim was to point at the same point on the outflow surface with a constant distance ℓ .

As the the possible mass flux is relatively low, due to the large outflow area, comparatively low dynamic pressure values were expected. To account for this, l=2 mm and l=3 mm were chosen. With an minimum allowable distance a of 0.2 mm between pitot tube and fin surface, this results in a smallest possible angle of α of 18.28° and 12.31°, respectively. An ideal choice would have been an $\alpha=6^{\circ}$,

$ \begin{array}{c ccccccccccccccccccccccccccccccccccc$	_	Case	Angle α [deg]	distance l [mm]	Case	Angle α [deg]	distance l [mm]	
3 45 2 mm 10 45 3 mm 4 60 2 mm 11 60 3 mm 5 75 2 mm 12 75 3 mm 6 90 2 mm 8 90 3 mm 7 96 2 mm 8 96 3 mm 7 96 2 mm 8 96 3 mm 18.28° 19.8	_	1	18.28	2 mm	8	12.31	3 mm	
4 60 2 mm 11 60 3 mm 5 75 75 2 mm 12 75 3 mm 6 90 3 mm 7 96 2 mm 8 90 3 mm 7 96 2 mm 8 96 3 mm 7 96 2 mm 8 96 3 mm 15, 7 96 2 mm 8 96 3 mm 7 96 2 mm 8 96 3 mm 15, 7 102, 7 89, 7 8	_	2	30	2 mm	9	30	3 mm	
$\begin{array}{c ccccccccccccccccccccccccccccccccccc$	_	3	45	2 mm	10	45	3 mm	
6 90 2 mm 8 90 3 mm 7 96 2 mm 8 96 3 mm 18.28° 18.28° 18.28° 18.28° 18.28° 18.28° 18.28° 18.28° 18.28° 18.28° 18.28° 18.28° 18.28° 18.28° 18.28° 18.28° 18.28° 10.14		4	60	2 mm	11	60	3 mm	
7 96 2 mm 8 96 3 mm 18.28° 10.2 $\frac{1}{440}$ 20.3 $\frac{1}{440}$ 20.3 $\frac{1}{440}$ 20.4 $\frac{1}{440}$ 20.5 $\frac{1}{440}$ 20.6 $\frac{1}{440}$ 20.7 $\frac{1}{440}$ 20.8 $\frac{1}$		5	75	2 mm	12	75	3 mm	
18.28° 19.8° 101.4°		6	90	2 mm	8	90	3 mm	
18.28° 19.67° 101.4		7	96	2 mm	8	96	3 mm	
45° -89,8 -79, -78,1 -66,4 -54,8 -66,4 -54,8 -77, -66,4 -43,1 -31,4 -31,	42 - 41 - 40 - E 39 - 33 - 37 - 36 -	336	338 340 34: x/mm	- 673,9 ed - 596,2 / 596,2 / 518,6 - 440,9 and - 363,2 285,6 - 207,9 ed - 130,2 pd - 52,625,1	45 - 44 - 43 - E 42 - 41 - 40 - 39 -	x / mm	- 102,7 - 89,7 & - 76,7 - 63,7 - 50,6 sance be - 37,6 - 24,6 - 11,6 - 11,6 1,4 14,4	
	51 - 50 - 49 - 48 - 47 - 46 - 45 -	336	, , , , , , , , , , , , , , , , , , ,	- 89,8 - 78,1 - 66,4 - 54,8 - 43,1 - 31,4 - 19,8 - 19,8 - 8,1 - 3,6 15,3	79 - 78 - 77 - EE 76 - 75 - 74 - 73 -		90° - 84,9	
(θ) ω 10			(c) $\alpha = 45^{\circ}$				= 90°	

Table 2. Investigated test cases with inclined pitot probe

Fig 7. Outflow distribution with different probe inclinations

due to the fin leading edge angle of 12° , and the pore structure defined by the aramid fiber fabric, as shown in Fig. 1b. The test cases investigated are shown in Table 2. Fig. 7 shows the outflow distribution measured for the same direct distance between the fin surface and the pitot tube l=2 mm and different angles relative to the fin surface α . Note that the smallest angle relative to the surface was chosen as $\alpha=18.28^{\circ}$. For this angular setting, as shown in Fig.7a a relatively high peak pressure could be measured, mostly dominated by a very strong jet, induced most probably by a very big pore or little defect in the structure. As shown in Fig.7b and Fig.7c, the jet is still visible, however, especially at $\alpha=30^{\circ}$, the jet expands relatively strongly, which is accompanied by significantly lower measured

dynamic pressures. For α = 90°, a negative pressure field was measured at the location of the jet, indicating a recirculation zone by the jet. For further investigation of the main outflow directions, the averaged pressures of the measured areas have to be considered. Fig. 8 shows the average pressure

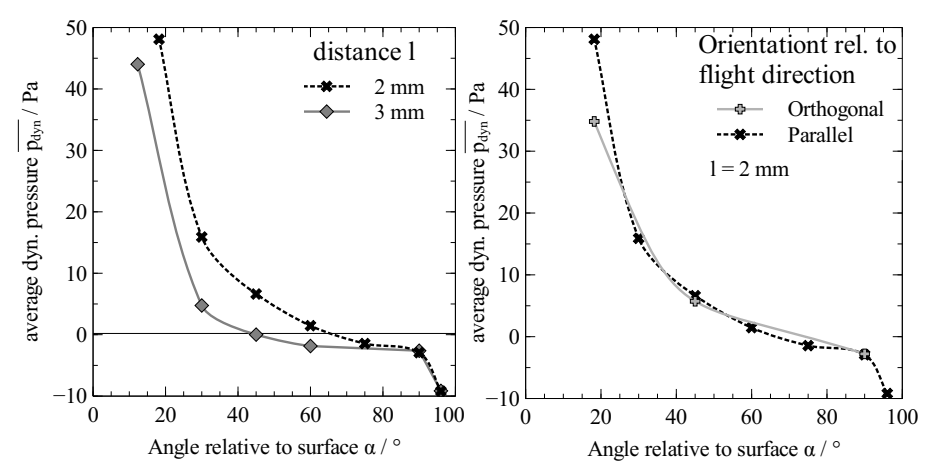


Fig 8. Directional dependency of outflow

values \bar{p}_{dyn} of the investigated measurement window for different pitot tube angles at l=2 mm and l=3 mm. These results are in accordance with the findings from Dittert et al. [9] for the investigations of a porous cone made of Carbon fiber reinforced Carbon (C/C). However, it has to be noted that the OCTRA material of the investigated fin has a more pronounced anisotropy compared to the C/C material. Parallel to the fiber direction, OCTRA has a significantly higher permeability compared to C/C with $K_{D,\parallel}=4.36\cdot 10^{-13}$ m². Furthermore, C/C has with $K_{D,\perp}=5.20\cdot 10^{-14}$ m² a significantly higher permeability than OCTRA, which is practically impermeable perpendicular to the fibre direction. Furthermore, the directional dependency of the outflow was investigated. The additional measurements were conducted, with the outflow direction orthogonal to the leading edge, oriented towards the fin tip. As shown in Fig.1b, these are expected to be the two main outflow directions due to the main orientation of the designed pore structure of the OCTRA material. The measurements were taken for $\alpha=18.28^{\circ}$, 45° and 90 °. For $\alpha=90^{\circ}$ and 45°, no significant influence on the average dynamic pressure could be found, having practically the same outflow behavior, whereas for $\alpha=18.28^{\circ}$, a significantly lower average pressure could be measured.

4.2. Outflow characterization of full fin

Based on the results presented in Section 4.1, a measurement of the whole port side of the fin was performed. For this study, α was kept at 18.28° and l was kept at 2 mm. Fig. 9 displays the outflow distribution measured over the whole outflow area. Generally, it can be seen, that low dynamic pressures are measured at the leading edge of the fin and close to the interface between the permeable OCTRA part and the impermeable C/C-SiC part. The latter effect can be explained by the highly anisotropic permeation properties of the OCTRA material. This part is nearly perpendicular to the plenum, hence the gas has to flow nearly perpendicular to the plenum through the porous medium to exit in this area. As OCTRA is practically impermeable perpendicular to the fiber plies, no outflow could be detected in that area. The low outflow rate near the leading edge of the fin can also be explained by geometric properties of the fin. Although the leading edge is aligned to the fiber direction, as seen in Fig. the perfusion length between the tip and the center area of the OCTRA part is significantly longer. Assuming constant plenum and ambient pressures, according to Eq.1 the mass flow rate is following the sharpest gradient, existent in the center part of the fin due to the short characteristic length. However, for application in hypersonic flight, such outflow characteristics are not desired, as the highest thermal loads are apparent at the sharp leading edge tip, requiring the most effective cooling and hence most outflow in this region. This can be solved through a improved fin design.

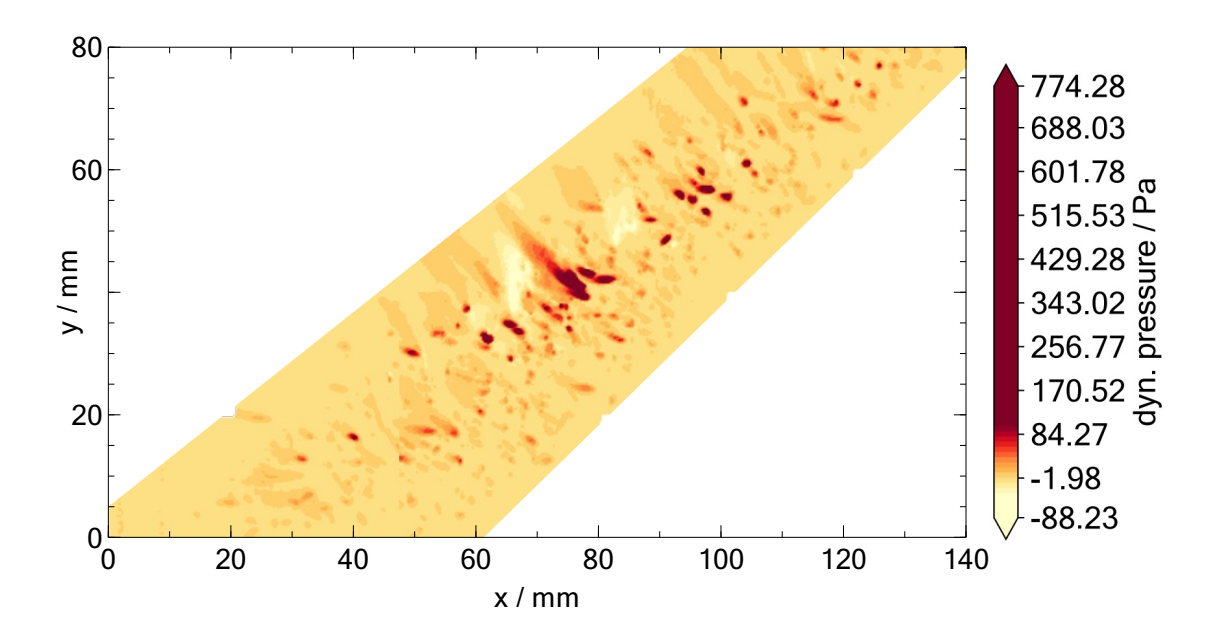


Fig 9. Outflow Distribution Whole Fin

5. Conclusion and Outlook

A study on the throughflow and outflow characteristics on a transpiration cooled CMC fin as flown on the HIFLIER sounding rocket flight experiment was conducted. While past characterizations of the outflow pattern focused on the investigation of simple geometries for fundamental research, this time a study was conducted on a more complex, realistic geometry for sounding rocket experiments. For the investigation of the general outflow pattern, a detailed study was conducted on a small 8 mm x 8 mm field in the center of the fin, with measurements at distances and angles to the specimen surface. As a result, the general outflow pattern could be shown as a low- dynamic pressure, relatively homogeneous outflow with disruptions by single strong jets caused by small inhomogeneities of the pore pattern. Furthermore, the strongly anisotropic permeability properties of the utilized porous CMC material could be successfully shown, being qualitatively similar to the results of the study conducted by Dittert et al.[9]. The outflow investigation of the whole fin showed that the highest mass flow rate is located at the center line, which can be explained by the combination of the fibre structure and lowest wall thickness. Due to the high wall thickness, almost no outflow could be measured at the fin's leading edge. However, this is not desired for fins for a hypersonic flight vehicles, as the sharp leading edge as the structure with the highest thermal load should be sufficiently cooled in order to maintain structural integrity of the sharp edge.

While the flight data obtained during the HIFLIER1 flight don't allow for a high-resolution spatial analysis of the cooling efficiency, plasma wind tunnel experiments on the fin will be performed. In such studies, the local cooling effect can be investigated by measuring the local wall temperature via IR cameras. In combination with the results from the outflow measurements, the effects of local coolant jets and recirculation zones on the cooling efficiency can be investigated. However, generally a high outflow homogeneity is desired.

From the results of the outflow investigations, three main factors for the improvement of the design of transpiration cooled can be extracted. Firstly, the general outflow behavior could be improved by employing more homogeneous materials or improving the homogeneity of the used CMC material. However, the exact effect on the cooling effectiveness is still under investigation.

Furthermore, the design of the fin has to be adapted in order to have a high mass flow rate at the leading

edge especially at the leading edge, which could be realized with a graded porosity pattern, leading to high permeablities at the leading edge and consequently a higher cooling mass flux. Concluding from the analysis of the outflow relative to the flight direction, it can be shown that a significant amount of coolant is flowing perpendicular to the flight direction. With an improved fin design, and the potential improvement of the material towards a single-directional pore structure, this potential source of coolant loss could also be minimized.

As a final conclusion, it could be shown that the investigation of the outflow pattern of a transpiration cooled structure plays a vital role in the improvement of the design for future thermally highly loaded spacecraft structures.

6. Acknowledgements

The authors like to thank Matthias Scheiffele and Felix Vogel from the Ceramic Composites and Structures department of DLR-BT, for the manufacturing of the raw materials, and Frank Entenmann from Space System Integration department of DLR-BT for the machining of the fin and for the continuous technical support.

References

- [1] J.D. Anderson Jr. Hypersonic and High-Temperature Gas Dynamics, 2006.
- [2] H. Böhrk. Transpiration cooling at hypersonic flight-AKTiV on SHEFEX II. In 11th AIAA/ASME Joint Thermophysics and Heat Transfer Conference, page 2676, 2014.
- [3] H. Böhrk, S. Löhle, U. Fuchs, H. Elsäßer, and H. Weihs. inEx–Fin Experiment on HIFiRE-5. In 7th ESA Aerothermodyanmics Symposium for Space Vehicles, 2011.
- [4] G. Di Martino, H. Böhrk, J. Schäfer, C. Müller, J. Peichl, F. Hufgard, C. Dürnhofer, and S. Löhle. Design of the Transpiration Cooled Fin Experiment FinEx II on HIFLIER1. In 2nd International Conference on High-Speed Vehicle Science Technology, Bruges, Belgium, 2022.
- [5] G. Di Martino, J. Peichl, F. Hufgard, C. Dürnhofer, and S. Löhle. Setup of flight experiment of transpiration cooled sharp edge fins on the sounding rocket HIFLIER1. In *Aerospace Europe Conference* 2023 10th EUCASS 9th CEAS, Lausanne, Switzerland, 2023.
- [6] G. Di Martino, J. Peichl, F. Hufgard, C. Dürnhofer, S. Löhle, and J. Göser. Transpiration Cooled Fin Flight Experiment FinExII on HIFLIER1. In *HiSST: 3rd International Conference on High-Speed Vehicle Science Technology, Busan, Korea*, 2024.
- [7] G. D Di Martino, J. Peichl, F. Hufgard, S. Duernhofer, C.and Loehle, and J. Goeser. Main flight data on transpiration cooled sharp edge fins in hypersonic conditions on the sounding rocket HIFLIER. *Aerospace Science and Technology*, 158:109895, 2025.
- [8] C. Dittert and M. Kütemeyer. OCTRA Optimized Ceramic for Hypersonic Application with Transpiration. In M. Singh et al., editor, Advances in High Temperature Ceramic Matrix Composites and Materials for Sustainable Development, volume 263 of Ceramic Transactions. John Wiley & Sons, Hoboken, 2017.
- [9] C. Dittert, M. Selzer, and H. Böhrk. Flowfield and pressure decay analysis of porous cones. *AIAA Journal*, 55(3):874–882, 2017.
- [10] A. Gülhan, D. Hargarten, M. Zurkaulen, F. Klingenberg, F. Siebe, S. Willems, G. Di Martino, and T. Reimer. Selected results of the hypersonic flight experiment STORT. *Acta Astronautica*, 211:333–343, 2023.
- [11] A. Gülhan, D. Neeb, T. Thiele, and F. Siebe. Aerothermal postflight analysis of the sharp edge flight experiment-II. *Journal of Spacecraft and Rockets*, 53(1):153–177, 2016.
- [12] A. Gülhan, F. Siebe, G. Requardt, H. Weihs, T. Laux, J. Longo, T. Eggers, J. Turner, A. Stamminger, and M. Hörschgen. The Sharp Edge Flight Experiment SHEFEX I-A Mission Overview. In 5th European Workshop on Thermal Protection Systems and Hot Structures, 2006.

- [13] S. Gulli and L. Maddalena. Characterization of complex porous structures for reusable thermal protection systems: effective-permeability measurements. *Journal of Spacecraft and Rockets*, 51(6):1943–1953, 2014.
- [14] H. S. Ifti, T. Hermann, M. McGilvray, L. Larrimbe, R. Hedgecock, and L. Vandeperre. Flow characterization of porous ultra-high-temperature ceramics for transpiration cooling. *AIAA Journal*, 60(5):3286–3297, 2022.
- [15] M.D.M. Innocentini, A.C. Rizzi Jr., L.A. Nascimento, and V.C. Pandolfelli. The pressure–decay technique for air permeability evaluation of dense refractory ceramics. *Cement and Concrete Research*, 34:293–298, 2004.
- [16] V. König, M. Rom, S. Müller, M. Selzer, S. Schweikert, and J. von Wolfersdorf. Numerical and experimental investigation of transpiration cooling with carbon/carbon characteristic outflow distributions. *Journal of Thermophysics and Heat Transfer*, 33(2):449–461, 2019.
- [17] T. Langener, J. von Wolfersdorf, M. Selzer, and H. Hald. Experimental investigation of transpiration cooling applied to C/C material. *International Journal of Thermal Sciences*, 54:70–81, 2005.
- [18] Y.-Q. Liu, Y.-B. Xiong, P.-X. Jiang, Y.-P. Wang, and J.-G. Sun. Effects of local geometry and boundary condition variations on transpiration cooling. *International Journal of Heat and Mass Transfer*, 62:362–372, 2013.
- [19] D. J. Munk, M. Selzer, H. Seiler, M. Ortelt, and G. A Vio. Analysis of a transpiration cooled LOX/CH4 rocket thrust chamber. *International Journal of Heat and Mass Transfer*, 182:121986, 2022.
- [20] J. Peichl, J. Munk, and M. Selzer. Development and Characterization of Additively Manufactured Metallic Porous Structures for Transpiration Cooling Applications. 11th European Conference for Aeronautics and Aerospace Sciences (EUCASS), Rome, Italy, 2025.
- [21] D. Prokein, C. Dittert, H. Böhrk, and J. von Wolfersdorf. Transpiration cooling experiments on a CMC wall segment in a supersonic hot gas channel. In *2018 International Energy Conversion Engineering Conference*, page 4696, 2018.
- [22] M. Selzer, H. Hald, S. Schweikert, and J. von Wolfersdorf. Measurements of surface exhalation characteristics of porous fibre reinforced composites. *4th International Conference on Porous Media and its Applications in Science and Engineering, Potsdam, Germany*, 2012.
- [23] M. Selzer, J. Peichl, I. D. Hoffmann, and D. Suslov. Outflow measurements on porous injector elements. Aerospace Europe Conference 2023 10th EUCASS 9th CEAS, Lausanne, Switzerland, 2023.
- [24] M. Selzer, S. Schweikert, H. Böhrk, H. Hald, and J. von Wolfersdorf. Comprehensive C/C sample characterizations for transpiration cooling applications. Annual report, Technical University of Munich, Garching, Germany, 2016.
- [25] M. Selzer, S. Schweikert, H. Hald, and J. von Wolfersdorf. Throughflow characteristics of C/C. Annual report, Technical University of Munich, Garching, Germany, 2014.
- [26] H. Weihs, J. Longo, and J. Turner. The sharp edge flight experiment SHEFEX II, a mission overview and status. In *15th AIAA International Space Planes and Hypersonic Systems and Technologies Conference*, page 2542, 2008.